

Multigram Scale, Solventless, and Diffusion-Controlled Route to Highly Monodisperse PbS Nanocrystals

Ludovico Cademartiri,[†] Jacopo Bertolotti,[‡] Riccardo Sapienza,[‡] Diederik S. Wiersma,[‡] Georg von Freymann,^{‡,§} and Geoffrey A. Ozin^{*,†}

Materials Chemistry Research Group, Lash Miller Chemical Laboratories, Department of Chemistry, University of Toronto, Toronto, Ontario, M5S 3H6 Canada, and European Laboratory for Non-Linear Spectroscopy (LENS) and INFN-MATIS, University of Florence, Polo Scientifico, Via Nello Carrara 1, I-50019, Sesto Fiorentino, Firenze, Italy

Received: November 3, 2005; In Final Form: December 12, 2005

High-quality PbS nanocrystals were produced in multigram-scale quantities through a solventless, heterogeneous, and relatively green route. The heterogeneous nature of this reaction allows one to limit the diffusion in the system, allowing for unprecedented monodispersity and quality of the product demonstrated by a full-width at half-maximum of the photoluminescence peak (PL fwhm) as low as 52 meV, a Stokes shift as low as 10 meV, and a quantum yield (QY) of 40%. The growth of the nanocrystals is interpreted in the framework of a diffusion-controlled Ostwald growth in conditions of strong supersaturation.

In recent years considerable effort has been dedicated to the development of reproducible syntheses of monodisperse lead chalcogenide nanocrystals (ncs).^{1–4} The interest in these materials is in fact encompassing a wide area of science and technology,⁵ especially after the discovery of their highly efficient multiple exciton generation,^{6,7} which could greatly enhance the efficiency of quantum-dot-based solar cells. For any research and application on these materials, it is highly desirable to have reproducible ways to obtain highly monodisperse nanocrystals, preferably through low-temperature, environmentally friendly, multigram-scale syntheses.⁸

PbCl₂ (98%) and technical grade oleylamine (OLA) (1:2 molar ratio) are magnetically stirred under N₂ flow in a round-bottom flask and heated to 100 °C when the flask is sealed and degassed under vacuum for 5 min. The flask is then reopened and the N₂ flux is restored while the temperature is increased to 120 °C and left there for 30 min. At the same time, sulfur is dissolved in OLA (0.1:0.2 molar ratio with respect to the PbCl₂ suspension) and the solution is put in an oven at 80 °C for 30 min. During this time the PbCl₂ suspension becomes highly viscous (higher PbCl₂:OLA ratios induce gelling of the suspension at ~120 °C). The sulfur–OLA solution is then quickly injected in the flask while the temperature is allowed to decrease to 100 °C where it is then kept for the growth of the nanocrystals. Once the desired size is achieved, the reaction is quenched by pouring the product in cold hexane. The solution is centrifuged to precipitate excess PbCl₂, the supernatant is precipitated with minimum amount of ethanol, and the precipitate is then redispersed in hexane. The excess sulfur precursor is separated with oleic acid and the nanocrystals are then further

washed thrice with ethanol before redispersing them in an apolar solvent. Up to 1.5 g of product can be obtained from a 50 mL reaction.

The PXRD analysis on the product confirms it to be single-phase PbS (Figure 1a). The TEM analysis (Figure 1b,c) confirms the high monodispersity and colloidal stability of the nanocrystals as they tend to form periodic superlattices. All the samples showed an isotropic spherical shape, and no transition to cubes, common for lead chalcogenide nanocrystals,^{3,10,11} has been observed for the size range investigated. This is consistent with the experimental results of Cho et al.¹¹ who found primary amines to preferentially coordinate the {111} facets of PbSe, thus preventing the formation of {100} terminated cubes. These nanocrystals can also undergo “nanocrystal plasma-polymerization”⁹ without losing their functionality to form flexible nanocrystal solids on plastic substrates (see Supporting Information). This characteristic was shared by all the samples produced with this synthesis.

As confirmed by ¹H NMR (Supporting Information), the capping group is the amine, which coordinates the surface Pb atoms with the nitrogen lone pair. XPS (Supporting Information) and elemental analysis confirm that the atomic ratio Pb/S is between 1.3 and 1.5, thus confirming the hypothesis of a Pb-rich surface. Charge balance is provided by Cl[−] ions adsorbed on the surface, which were detected by XPS and EDAX in an atomic percentage equal to 50–60% with respect to Pb (Supporting Information). No peak corresponding to a PbCl₂ phase was detected in the PXRD, and no extraneous crystallites were seen during TEM analysis. We can then exclude the presence of a nanocrystalline form of PbCl₂, which would appear as an amorphous halo in the PXRD, especially considering the overall concentration of Cl detected. From the obtained values of concentration and considering the surface-to-bulk ratio in our quantum dots, we estimated a thickness for this lead-

* Corresponding author. E-mail: gozin@chem.utoronto.ca

[†] University of Toronto.

[‡] University of Florence.

[§] Present address: Institut für Angewandte Physik, Universität Karlsruhe (TH), 76128 Karlsruhe, Germany

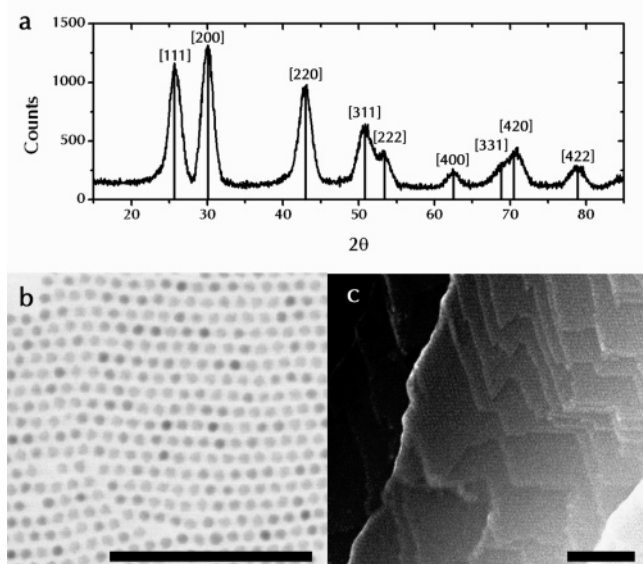


Figure 1. (a) PXRD of a PbS sample with vertical lines indicating the positions of the peak in bulk PbS. (b) TEM of a monolayer of PbS nanocrystals arranged in hexagonal packing; (c) TEM of a plasma-polymerized PbS nanocrystal superlattice obtained by slowly drying an hexane solution of nanocrystals and exposing the resulting film to plasma treatment.⁹ Scale bars are 100 nm.

chloride-like shell of ~ 4 Å, which is comparable to the length of a Pb–Cl bond (2.5–3.5 Å depending on the type of bonding). It is not clear at the moment from our results what is the precise nature of the bond between Pb and Cl at the surface, as we could not extract unequivocal information from the high-resolution XPS of the Pb 4f peak or the Cl 2p peak.

The PbCl_2 –OLA system is a unique system for the synthesis of lead chalcogenide nanocrystals as PbCl_2 forms a suspension in OLA. It is the first time to our knowledge that a heterogeneous system has been adopted for the synthesis of semiconductor nanocrystals through a “hot injection” method. The viscosity of the growth environment can be continuously tuned by changing the PbCl_2 :OLA ratio and thus by thickening the suspension. By increasing the viscosity of the system, and with it decreasing the mass-transfer coefficient, the nanocrystals are coerced to grow in a more diffusion-controlled reaction, which has been shown to be one of the prerequisites for the enhancement of the “focusing” of the nanocrystals size distribution¹² (narrowing of the size distribution of colloids during growth) and for delaying the occurrence of the classical Ostwald ripening.¹² By reacting “pure” precursors (the nature of the Pb precursor is at this stage still not completely clear), we substantially increased the supersaturation at the time of injection, which was found to lead to a pronounced focusing of the nanocrystal size distribution.¹² In the case of cadmium chalcogenides, the increase of the concentration of the precursor leads to the formation of anisotropic nanoparticles,¹³ which have not been observed in our system probably due to the isotropy of the NaCl-like lattice of PbS and to the use of a single ligand. By reacting “pure” precursors we also avoided the use of solvents or excess ligands, which inevitably would increase the cost and environmental unfriendliness for large-scale production. The widespread use of noncoordinating solvents such as octadecene¹⁴ for the synthesis of nanocrystals might not in fact be cost-effective for the industrial scale production of nanocrystals. We calculated the price of PbS nanocrystal produced with this synthesis to be approximately \$14 (U.S.) per gram by considering raw materials and solvents, including purification.

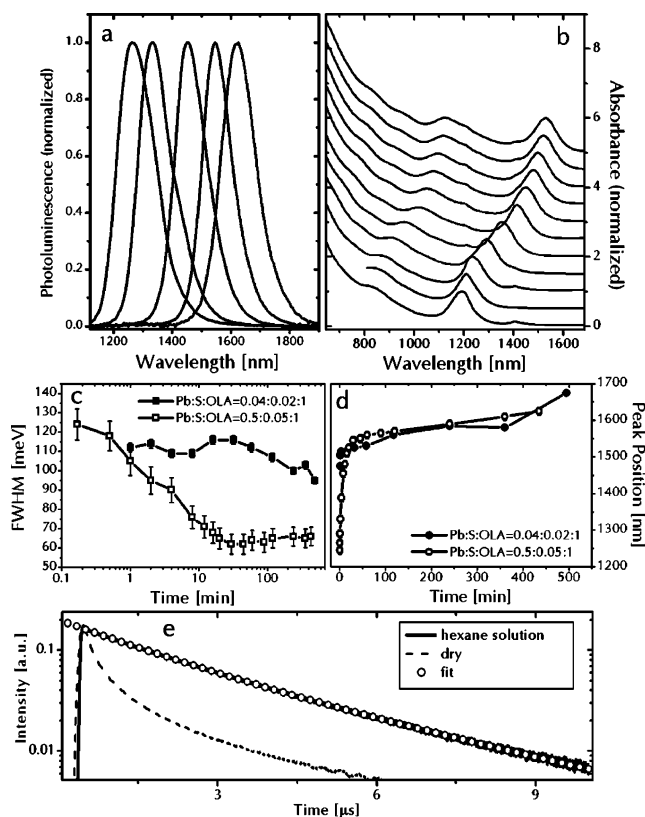


Figure 2. (a) Photoluminescence (PL) of PbS ncs during growth. (b) Absorption of PbS ncs during growth (the small features at 1200 nm and 1400 nm are artifacts). (c) Evolution of the PL fwhm during the growth for different PbCl_2 :S:OLA ratios; abscissa is in logarithmic scale. (d) Evolution of PL peak position during the growth for different PbCl_2 :S:OLA ratios. (e) PL lifetime of PbS nanocrystals in hexane (solid — exponential fit indicated with empty circles) and dry (dashed).

As shown in Figure 2 we were able to reproducibly obtain PbS nanocrystals emitting from 1245 to 1625 nm with a fwhm of the PL peak as low as 62 meV (preliminary results indicate that it is possible to reach values of ~ 50 meV; see Supporting Information) and with no trace of trap-related emission up to 2100 nm. This result brings the quality of PbS nanocrystals to the levels obtained for PbSe nanocrystals where a fwhm of the PL below 70 meV are sometimes reported.^{15,16} The quantum yield was measured by using the dye IR-125 as a standard and was found to be up to $\sim 40\%$, while the Stokes shift decreased to ~ 10 meV during focusing (see Supporting Information), confirming the high quality of the nanocrystals and the efficient capping of their surface provided by the amines. The photoluminescence lifetime for nanocrystals in solution and dried was measured under excitation at $1.064 \mu\text{m}$ (Figure 2e). In contrast with previous reports¹⁷ on lead sulfide nanocrystals, the photoluminescence lifetime in hexane was found to be $1.828 \mu\text{s}$, instead of $1 \mu\text{s}$. In the dried state it becomes nonexponential and shorter because of Förster energy transfer between neighboring nanocrystals. These long lifetimes in solution can be explained by considering the dielectric screening effects, which are particularly pronounced in lead chalcogenide nanocrystals due to their high dielectric constant ($\epsilon = 17$ for PbS).^{18,19} As our value of lifetime is in almost quantitative agreement with what is expected for dielectric screening effects,²⁰ the dielectric constant of these nanocrystals can be considered very close to the bulk value.

As shown in Figure 2c, when PbCl_2 :OLA = 0.5, the initial distribution focuses dramatically (the PL fwhm usually halves during focusing) and then stabilizes at 62–65 meV with almost

no sign of subsequent broadening. The PL peak position evolution during the reaction also shows two distinct regions in which the shift is more or less linear in time but with drastically different slopes. In the first region the high concentration of available precursors generates a fast growth, which then abruptly slows down as soon as the supersaturation diminishes, and further growth is achieved by ripening (even though we do not observe substantial broadening of the PL peak even after hours of growth). The point of maximum focusing can be found at the intersection of these two regions. It is worth noting that the dependence of PL peak position vs nanocrystal size is nonlinear so that the linear trends shown in Figure 2d would not be such in a diameter vs time plot. When $\text{PbCl}_2\text{:OLA} = 0.04$, the initial size distribution remains broad (PL fwhm ~ 100 meV) and approximately constant, suggesting that the reaction reaches very quickly the stationary regime (corresponding to a polydispersity of $\sim 20\%$)¹² predicted by the theory of Lifshitz and Slyozov²¹ and Wagner²² for an ensemble of particles undergoing Ostwald ripening.²³

This entire behavior is consistent with the computational results of Talapin et al.¹² in which a low mass-transfer coefficient and a high supersaturation of the monomer during the growth stage were found to be the best conditions for the growth of monodisperse nanocrystals. We use pure and highly viscous precursors to increase the supersaturation and reduce the mass-transfer coefficient while the high ratio between them ($\text{Pb:S} = 10:1$) amplifies the effects of the limited diffusion. The excess of Pb is in fact limiting the decrease of supersaturation during the growth, thus prolonging the “focusing region” of the reaction which strongly depends on the supersaturation.¹² Since the critical radius is inversely proportional to the logarithm of the supersaturation, this also means that the critical radius increases more slowly than for a stoichiometric ratio of precursors. This slower increase of the critical radius then delays the initiation of the classical Ostwald ripening, which would bring the size distribution back to the steady-state regime (polydispersity $\sim 20\%$). This is further confirmed by the higher monodispersity and smaller nanocrystals at high ratios of Pb:S .⁴

When $\text{PbCl}_2\text{:OLA} = 0.04$ instead, the supersaturation is much smaller and most of the precursors are consumed during the nucleation event so that further growth can only be achieved by dissolution of the smaller particles. In other words, the supersaturation during growth is in this case very low, if any, and the critical radius increases to the point of being comparable with the average nanocrystal size, thus initiating the ripening process.

We still cannot fully explain within the limitations of this framework why the PL fwhm for $\text{PbCl}_2\text{:OLA} = 0.5$ stabilizes at such low values instead of increasing rapidly as predicted by the steady-state distribution upon termination of the focusing phase.¹² Our interpretation is that the high precursor ratio used keeps the supersaturation high, even at later stages of the reaction when the S precursor is almost completely depleted, thus preventing Ostwald ripening from effectively initiating. At

this point it is worth noting that the Monte Carlo simulations included in the paper by Talapin et al.¹² were performed considering soluble precursors and a solvent-based synthesis. Our reaction would probably not be simulated in the best way with the parameters chosen for those simulations since they would not consider, for example, the different kinetics involved in a heterogeneous reaction such as the one described here.

Acknowledgment. G.A.O. is Canada Research Chair in Materials Chemistry. The authors are deeply indebted to NSERC and the network of excellence Phoremest for financial support. The authors are also grateful to Frank W. Wise for valuable discussion.

Supporting Information Available: Experimental details; evolution of Stokes Shift and half-width at half-maximum on the low energy side (HWHM) of 1st exciton peak in the absorption spectrum during growth; 52 meV-wide PL peak; photo and SEM of a flexible PbS nanocrystal solid; ^1H NMR of PbS OLA-capped nanocrystals and OLA; XPS of highly purified PbS nanocrystals with respective compositional analysis. This material is available free of charge via the Internet at <http://pubs.acs.org>.

References and Notes

- (1) Hines, M. A.; Scholes, G. D. *Adv. Mater.* **2003**, *15*, 1844.
- (2) Bakueva, L.; Gorelikov, I.; Musikhin, S.; Zhao, X. S.; Sargent, E. H.; Kumacheva, E. *Adv. Mater.* **2004**, *16*, 926.
- (3) Joo, J.; Na, H. B.; Yu, T.; Yu, J. H.; Kim, Y. W.; Wu, F.; Zhang, J. Z.; Hyeon, T. *J. Am. Chem. Soc.* **2003**, *125*, 11100.
- (4) Cademartiri, L.; von Freymann, G.; Kitaev, V.; Ozin, G. A. *AIP Conf. Proc.* **2005**, *772*, 597.
- (5) Wise, F. W. *Acc. Chem. Res.* **2000**, *33*, 773.
- (6) Schaller, R. D.; Klimov, V. I. *Phys. Rev. Lett.* **2004**, *92*, 186601.
- (7) Ellingson, R. J.; Beard, M. C.; Micic, O. I.; Nozik, A. J.; Johnson, J. C.; Yu, P.; Shabaev, A.; Efros, A. L. *Nano Lett.* **2005**, *5*, 865.
- (8) Peng, X. *Chem.-Eur. J.* **2002**, *8*, 334.
- (9) Cademartiri, L.; von Freymann, G.; Arsénault, A. C.; Bertolotti, J.; Wiersma, D. S.; Kitaev, V.; Ozin, G. A. *Small* **2005**, *1*, 1184.
- (10) Lu, W.; Fang, J.; Stokes, K. L.; Lin, J. *J. Am. Chem. Soc.* **2004**, *126*, 11798.
- (11) Cho, K.-S.; Talapin, D. V.; Gaschler, W.; Murray, C. B. *J. Am. Chem. Soc.* **2005**, *127*, 7140.
- (12) Talapin, D. V.; Rogach, A. L.; Haase, M.; Weller, H. *J. Phys. Chem. B* **2001**, *105*, 12278.
- (13) Peng, X.; Manna, L.; Yang, W.; Wickham, J.; Scher, E.; Kadavanich, A.; Alivisatos, A. P. *Nature* **2000**, *404*, 59.
- (14) Qu, L.; Peng, Z. A.; Peng, X. *Nano Lett.* **2001**, *1*, 333.
- (15) Pietryga, J. M.; Schaller, R. D.; Werder, D.; Stewart, M. H.; Klimov, V. I.; Hollingsworth, J. A. *J. Am. Chem. Soc.* **2004**, *126*, 11752.
- (16) Coe-Sullivan, S.; Bulovic, V.; Steckel, J. S.; Woo, W.-K.; Bawendi, M. G. *Adv. Funct. Mater.* **2005**, *15*, 1117.
- (17) Warner, J. H.; Thomsen, E.; Watt, A. R.; Heckenberg, N. R.; Rubinsztein-Dunlop, H. *Nanotechnology* **2005**, *16*, 175.
- (18) Wehrenberg, B. L.; Wang, C.; Guyot-Sionnest, P. *J. Phys. Chem. B* **2002**, *106*, 10634.
- (19) Du, H.; Chen, C.; Krishnan, R.; Krauss, T. D.; Harbold, J. M.; Wise, F. W.; Thomas, M. G.; Silcox, J. *Nano Lett.* **2002**, *2*, 1321.
- (20) Wise, F., personal communication.
- (21) Lifshitz, I. M.; Slyozov, V. V. *J. Phys. Chem. Solids* **1961**, *19*, 35.
- (22) Wagner, C. Z. *Elektrochem.* **1961**, *65*, 581.
- (23) Ostwald, W. Z. *Phys. Chem.* **1901**, *37*, 385.